RAA 2018 Vol. **18** No. **8**, 102(6pp) doi: 10.1088/1674–4527/18/8/102

http://www.raa-journal.org *http://iopscience.iop.org/raa*

Research in Astronomy and Astrophysics

Cooling and energy loss of partially ionized hydrogen gas behind a shock wave

Oksana Mikhailovna Belova[1,2] and Konstantin Veniaminovich Bychkov[2]

[1] Faculty of Physics, Lomonosov Moscow State University, Leninskiye Gory, 1-2, Moscow, 119991, Russia; *whitecanvas05122010@mail.ru*

[2] Sternberg Astronomical Institute, Lomonosov Moscow State University, Universitetsky pr., 13, Moscow, 119234, Russia

Received 2017 November 29; accepted 2018 April 18

Abstract We studied the difference in behavior of total energy and its thermal component during the radiative cooling of partially ionized hydrogen gas. Our calculations were fulfilled for the conditions in the atmosphere of a cool star. It is shown that the attenuation of total energy loss does not interfere with the cooling rate.

Key words: stellar atmospheres: shock wave

1 INTRODUCTION

Gorbatskii (1961) suggested the model of a radiative shock wave for solving the problem of bright lines in the spectra of Mira type stars. He took into account the difference between the electron temperature $T_{\rm e}$ and the temperature of hydrogen atoms and protons $T_{\rm ai}$. The multiple scattering of Lyα radiation was investigated in a two-level model. Later the problem was considered by Fox & Wood (1985). They used a ten-level model of hydrogen supposing that all plasma components — atoms, ions, and electrons — have a single value of current temperature. Fadeyev & Gillet (2000, 2004) solved the problem in a two-temperature approach including a five-level model. Belova et al. (2014) considered a more realistic 25 level model of a hydrogen atom, according to the Inglis–Teller equation, in a two-temperature approach. As follows from the shock wave calculation, for example Fadeyev & Gillet (2004) and Belova et al. (2014), the Lyman and Balmer lines are locked in the cooling region. The multiple scattering of radiation in the frequencies of discrete transitions increases the population of excited states.

In this paper we investigate some features of radiative cooling behind the shock wave by comparing the cooling rate to total energy loss due to radiative processes. In the literature (for example, Kaplan & Pikel'Ner 1979), the cooling function is used to describe the radiative loss. It is useful in "quasi stationary" processes when ionization and recombination compensate each other at the current value of slowly varying temperature. In this case, the radiative loss is equal to the cooling rate. The other situation takes place behind the shock wave where non-stationary processes occur. The gas heated by the viscous jump is being excited and ionized by electron impact. Both processes effect the electron temperature without altering the total energy.

2 COOLING, HEATING AND TOTAL ENERGY LOSS

Let us introduce the total energy loss rate L as the difference between the radiative loss rate $L_{\rm L}$ and the energy input rate $L_{\rm I}$ from a photosphere

$$L = L_{\rm L} - L_{\rm I}, \tag{1}$$

where

$$L_{\rm L} = \sum_{u>l} A^*_{ul}\left(1 + n^*_\omega(\nu_{lu})\right) E_{lu} \upsilon_u + N_{\rm e} x \sum_k R_k, \tag{2}$$

and

$$L_{\rm I} = 4\pi \left[\sum_{l<u} B_{lu} \cdot n^*_\omega(\nu_{lu}) \cdot E_{lu} \upsilon_l + \sum_k P_k \upsilon_k\right]. \tag{3}$$

Here indices l, u and k are values of principal quantum number, E_{lu} is the energy gap between levels; $N_{\rm e}$ is the electron number density; x is the hydrogen ionization degree, $\upsilon_k = N_k/N_{\rm H}$ is the relative population in the k-th state, and $N_{\rm H}$ is the total number density of protons and hydrogen atoms. The relation between the radiative transition probability A_{ul} and the Einstein absorption coefficient B_{lu} is $B_{lu} = (u/l)^2 A_{ul}$. The photon occupation number is designated as $n_\omega(\nu)$. For photospheric radiation, we use the diluted blackbody approximation

$$n_\omega(\nu) = \frac{W}{e^{h\nu/k_{\rm B}T_{\rm ph}} - 1},$$

where W is the dilution factor equal to 1/2, $T_{\rm ph}$ is the temperature of the photosphere and $k_{\rm B}$ is Boltzmann's constant. Symbol "$*$" means that the escape probability w_{lu} is taken into account with $A^*_{ul} = A_{ul} \cdot w_{lu}$ and $n_\omega(\nu_{lu})^* = n_\omega(\nu_{lu}) \cdot w_{lu}$; the summation is over all u and l such that $u > l$. The value of w_{lu} is calculated in the frame of the Biberman–Holstein approximation (Biberman et al. 1982). The line profile is caused by the Doppler shift in the rather rarefied atmosphere of a giant star like Mira Ceti ($N_{\rm e} < 10^{13}$ cm^{-3}), hence it follows that

$$w_{lk} = \left(2\tau_{lk} \cdot \sqrt{\pi \ln \tau_{lk}}\right)^{-1},$$

where τ_{lk} is the optical depth at the center of the line.

The energy input by photoionization is equal to

$$P_k = W \cdot g_k \int_{\nu_k}^{\infty} \sigma_k(\nu) B_\nu(T_{\rm ph})\, d\nu.$$

The Kramers' approximation is used for the photoionization cross section σ_k; $B_\nu(T_{\rm ph})$ is the Plank function. Factor g_k is equal to $e^{-\eta_1}$ for $k = 1$ and $g_k = 1$ for $k>1$, where η_k is the optical depth at the photoionization edge.

The symbol R_k designates recombination loss per one electron–proton pair,

$$R_k = (1 + \eta_k)^{-1} \times \int_0^{\infty} s_k v h\nu\, (1 + n_\omega)\, f(\varepsilon)\, d\varepsilon.$$

$$h\nu = \varepsilon + \chi_k.$$

The multiplier before the integral accounts for scattering at the threshold frequency for photoionization. Here s_k is the recombination cross section calculated from σ_k, χ_k is the ionization potential of the level k, $f(\varepsilon)$ is the Maxwellian distribution function on the electron energy ε and v is the free electron velocity. Our calculations (Sect. 5 of this paper) show that the cooling gas is opaque at the threshold frequency for photoionization from the ground level and it is transparent for other series.

The cooling rate C is defined as the difference between the rate of thermal energy loss C_C and the rate of its gain C_H

$$C = C_C - C_H. \tag{4}$$

Here C_C includes

– electron impact excitation

$$C_{\rm ex} = N_{\rm e} \cdot \sum_{l<u} q_{lu} \upsilon_l E_{lu}, \tag{5}$$

– impact ionization

$$C_{\rm ion} = N_{\rm e} \cdot \sum_k q_k \chi_k \upsilon_k,$$

– and photorecombination

$$C_{\rm rec} = N_{\rm e} N_{\rm p} \left(R_k - \chi_k \frac{r_k}{1 + \eta_k}\right),$$

where r_k is the recombination coefficient

$$r_k = \int_0^{\infty} s_k v\, (1 + n_\omega)\, f(\varepsilon)\, d\varepsilon.$$

The heating rate C_H is the sum of

– electron impact deactivation

$$H_{\rm deact} = N_{\rm e} \cdot \sum_{l<u} q_{ul} \upsilon_u E_{lu}, \tag{6}$$

– photoionization

$$H_{\rm photion} = W \times \sum_k g_k \upsilon_k \times \int_{\nu_k}^{\infty} \sigma_k(\nu) \frac{B_\nu(T_{\rm ph})}{h\nu}\, (h\nu - \chi_k)\, d\nu,$$

– and triple recombination

$$H_{\rm triple} = N_{\rm e}^2 x \sum_k \gamma_k \chi_k.$$

The impact rates q_{lu} and q_k were taken from Johnson (1972). The triple recombination coefficients γ_k were calculated from q_k using the principle of detailed balancing.

3 CASE WHEN ENERGY LOSS IS EQUAL TO HEATING RATE

Let us show that energy loss is equal to the cooling rate in stationary conditions. Consider a simplified case when the effects of free-bound processes and photospheric radiation are omitted ($W = 0$, $R_k = r_k = C_{\rm ion} =$

$H_{\rm triple} = 0$). $\upsilon_k^{\rm (s)}$ is designed as the solution of a stationary system of equations

$$\begin{aligned}&\left[\sum_{l<k}(A^*_{kl}+q_{kl}N_{\rm e})+\sum_{u>k}q_{ku}N_{\rm e}\right]\upsilon_k^{\rm (s)}\\&-\sum_{u>k}(A^*_{uk}+q_{uk}N_{\rm e})\,\upsilon_u^{\rm (s)}\\&-\sum_{l<k}q_{lk}N_{\rm e}\upsilon_l^{\rm (s)}=0.\end{aligned} \tag{7}$$

The balance Equation (7) causes the identical one

$$L_{\rm L}^{\rm (s)} = C_{\rm ex}^{\rm (s)} - C_{\rm deact}^{\rm (s)}. \tag{8}$$

It means that the radiative loss is equal to the difference between the excitation cooling and the deactivation heating rates. There is no question here of the relationship between the loss of total energy and its thermal component, since they are equal to each other.

The situation is more varied when partially ionized hydrogen is irradiating behind a shock wave. For example, the inequality

$$L<C \tag{9}$$

takes place, as follows from our direct calculations (Belova et al. 2014), for a shock velocity less than 100 km s^{-1}. This problem is investigated in detail.

4 NON-STATIONARY COOLING CALCULATIONS

Behind the shock front, the hydrogen ionization degree and the relative population of discrete levels are nonstationary. They can be found by solving the system of equations:

$$\begin{aligned}\frac{d\upsilon_k}{dt} = -\Bigg[&q_kN_{\rm e}+p_k\\&+\sum_{k<u}(q_{ku}N_{\rm e}+B_{ku}\cdot n^*_\omega(\nu_{ku}))\\&+\sum_{k>l}(A^*_{kl}\,(1+n^*_\omega(\nu_{lk}))+q_{kl}N_{\rm e})\Bigg]\upsilon_k\\&+(r_k+\gamma_kN_{\rm e})N_{\rm e}x\\&+\sum_{u>k}(A^*_{uk}\,(1+n^*_\omega(\nu_{ku}))+q_{uk}N_e)\,\upsilon_u\\&+\sum_{l<k}(B_{lk}\cdot n^*_\omega(\nu_{lk})+q_{lk}N_{\rm e})\,\upsilon_l,\end{aligned} \tag{10}$$

where p_k is the photoionization rate

$$p_k = 4\pi W\cdot g_k\int_{\nu_k}^{\infty}\frac{B_\nu(T_{\rm ph})}{h\nu}\sigma_k(\nu)\,d\nu.$$

The relative populations υ_k and x obey the normalization condition

$$\sum_k \upsilon_k + x = 1. \tag{11}$$

The equations for the heat energy and the electron temperature were given in Belova et al. (2014). The preshock temperature T_0 is assumed to equal 3200 K, the gas number density N_0 is 10^{12} cm^{-3}, the ionization degree is determined by the Saha equation at temperature T_0 and the shock velocity u_0 is 50 cm s^{-1}. The equations for electron temperature and thermal energy were solved by the explicit Euler scheme. The system of Equations (10)–(11) is solved using the implicit Eulerian scheme, while the iterations are performed using the Newton method.

5 EFFECT OF SCATTERING IN SPECTRAL LINES

The solid lines in Figure 1 represent the radiation loss rate L and the cooling rate C behind the shock front.

The dashed curve describes the evolution of the electron temperature $T_{\rm e}$ over a given time span. It is clearly seen that the cooling rate C exceeds the radiative loss rate L. At first, the difference is small, then it grows with time and reaches one order of magnitude at the moment of maximum electron temperature. The significant discrepancy between C and L is maintained during the time of the bulk of radiative energy loss.

Figure 2 illustrates the effect of scattering on the total energy loss.

This shows the dependence on time of optical depths in Lyα, Hα, Hβ, Pα and at the Lyman and Balmer limits. The Lyman lines and continuum radiation are locked almost immediately after the front passes. The shocked gas remains transparent for a long time in the Balmer lines. At the late stage of radiative energy loss, the scattering in lines of this series becomes significant.

The effect of electron impact ionization and deactivation on emission in lines is illustrated by the relation Ω_{ul}

$$\Omega_{ul} = \frac{(q_{ul}+q_u)N_{\rm e}}{A^*_{ul}} \tag{12}$$

which we call the "attenuation factor." The value of $1/\Omega_{ul}$ gives the approximate evaluation of the escape probability at $\Omega_{ul}>1$. The escape probability is close to one at $\Omega_{ul}<1$.

Figure 3 represents Ω_{ul} as a function of time for Lyα, Hα, Hβ and Pα. It is plainly seen that the energy

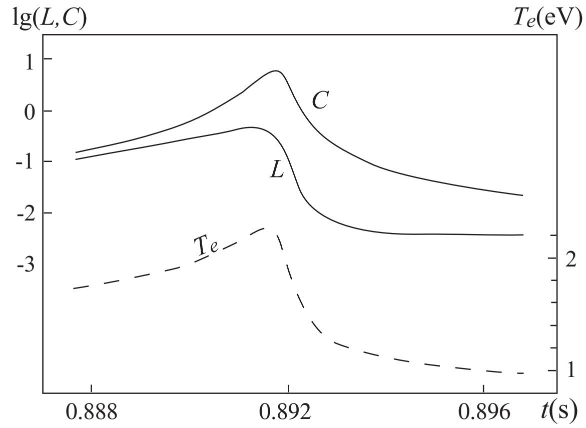

Fig. 1 Radiative energy loss rate (L) and cooling rate (C); the *dashed line* shows the time dependence of $T_{\rm e}$.

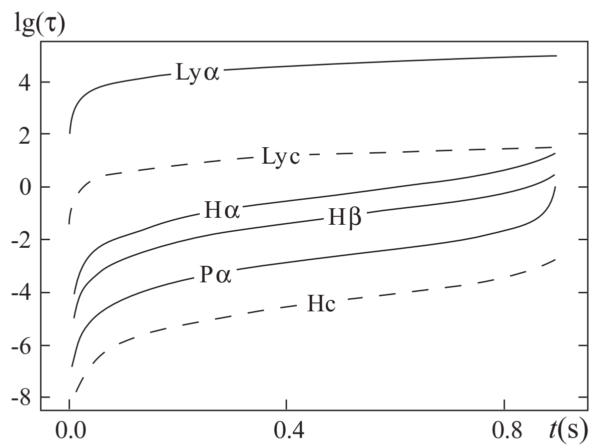

Fig. 2 Optical depths in Lyα, Hα, Hβ, Pα and at the Lyman and Balmer limits as functions of time t.

loss in Lyα is reduced approximately 100 times compared to the moment of maximum electron temperature. The radiation energy is transformed into internal (q_u) and thermal (q_{ul}) gas energy. In the case of transparent gas, the radiative loss is defined mainly by Lyα emission. Hence, the attenuation of energy loss is close to the one of Lyα; it is obvious when comparing the L-line in Figure 1 with the Lyα-line in Figure 3.

The input of different spectral series and photorecombination in the radiative loss L is shown in Figure 4: Lyman Ly, Balmer H, Paschen P, and Brackett Br; letter Σ designates the input of all others spectral series from Pfund ($l = 5$) till $l = 14$.

It is clearly seen that the Balmer and Paschen lines determine radiative loss. The Brackett lines are about an order of magnitude weaker. The total input of higher series is even smaller. The Lyman lines, which are the strongest lines in the spectra of many cosmic objects, are weaker here than the Balmer and Paschen ones by more than two orders of magnitude.

6 GAS COOLING WHEN LINE RADIATION IS LOCKED

We introduce the parameter $\varkappa$, which is equal to the ratio of the heating rate by deactivation to the cooling one by excitation

$$\varkappa = \frac{H_{\rm deact}}{C_{\rm ex}}, \tag{13}$$

which describes the return of thermal energy. The value of $\varkappa$ differs less than 5% from the full ratio $C_{\rm H}/C_{\rm C}$. If we fix the lower level l and sum Equations (5) and (6) over all upper levels u, we obtain the value $\varkappa_l$ for the

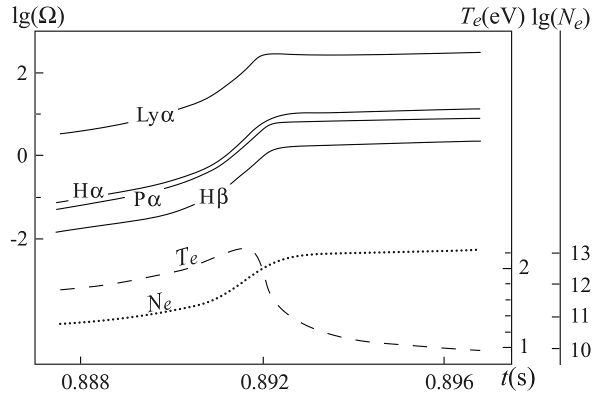

Fig. 3 *Solid lines* represent the dependence of Ω on time for Lyα, Hα, Hβ and Pα; *dashed curve* is the evolution of electron temperature T_{e}; the *dotted one* is the electron number density N_{e}.

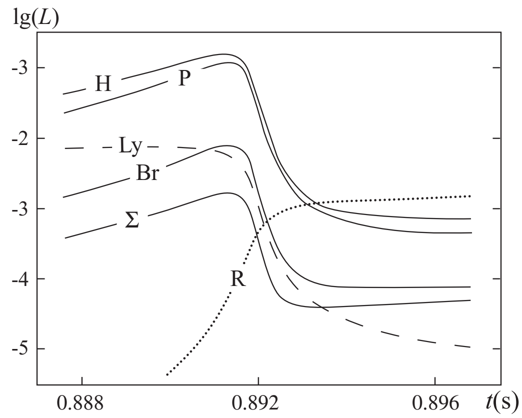

Fig. 4 The input of different spectral series of hydrogen atom into radiative energy losses L: Ly — Lyman, H — Balmer, P — Paschen, Br — Brackett, Σ — the total input of other series; R is the input of photorecombination.

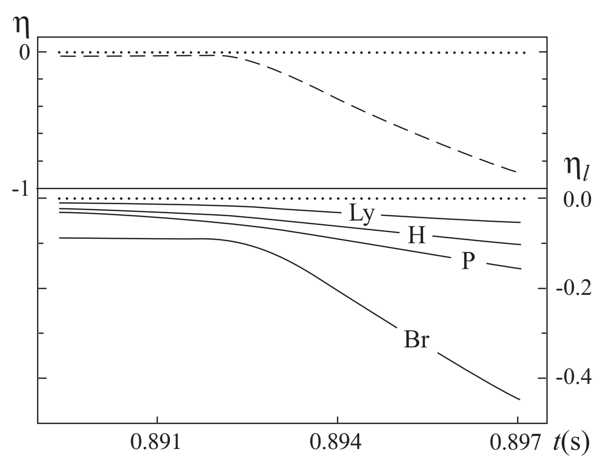

Fig. 5 The evolution of deactivation by electron impact: η — total effect, η_l — input of series from Ly to Br.

corresponding spectral series

$$\varkappa_l = \frac{\sum\limits_{u>l} q_{ul} \upsilon_u E_{lu}}{\upsilon_l \sum\limits_{u>l} q_{lu} E_{lu}}. \qquad (14)$$

At small values of $\varkappa$ and $\varkappa_l$, the logarithmic representation is useful

$$\eta = \lg(1-\varkappa), \qquad \eta_l = \lg(1-\varkappa_l). \qquad (15)$$

The values of η and η_l are illustrated in Figure 5.

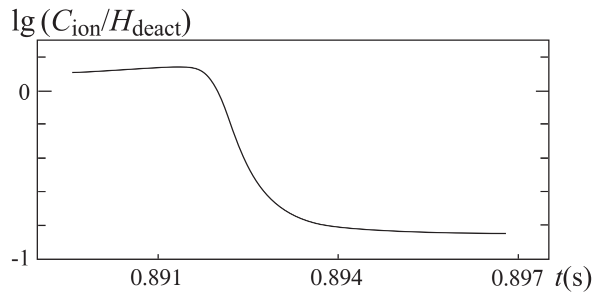

Fig. 6 The effect of ionization on cooling.

At the top of the figure is the dashed line representing η, and in its lower part are the values of η_l for the spectral series from Lyman ($l = 1$) till Brackett ($l = 4$). The effectiveness of the return of thermal energy due to deactivation is small during the time span from passing the front till the electron temperature maximum at $t < 0.892$ s. From this moment, $\varkappa$ begins to grow up to 90%. Thus, the total loss of C is at least 10% of $C_{\rm ex}$. It was previously shown that the radiative energy loss is reduced approximately 100 times. Hence, the value of L must be lower than C by about one order of magnitude, as is seen in Figure 1. In other words, the total energy loss is weakened to a greater extent than the cooling rate.

More detailed information showing the behavior of individual spectral series is presented in the lower part of Figure 5. In the first three spectral series, deactivation is insignificant, but its effect increases monotonically at higher values of l.

The decrease of ten times by C in Figure 5 is connected with the value of the ratio $C_{\rm ion}/H_{\rm deact}$, which is shown in Figure 6. This ratio tends to 0.1 which means that only 10% of the thermal energy is converted into internal energy.

7 CONCLUSIONS

It is necessary to take the ionization from excited states into account when calculating the radiative cooling behind a shock wave propagating through partially ionized hydrogen gas.

The radiation loss rate during non-stationary cooling can be significantly less than the cooling rate. The main cause is ionization by electron impact from excited states. The physical meaning is that ionization by electron impact does not affect the total energy of gas: the thermal energy of electrons is pumped to the internal energy of hydrogen atoms. As a result, the thermal energy decreases rapidly. At the same time the total energy loss, which is due only to the radiation, may be small in the case of locked radiation. The contents of our paper are reviewed in Samus & Li (2018).

References

Belova, O. M., Bychkov, K. V., Bychkov, E. S. & Morchenko, E. S. 2014, Astronomy Reports, 91, 745 (in Russian)
Biberman, L. M., Vorob ev, V. S., & Yakubov, I. T., Kinetika Neravnovesnoi Nizkotemperaturnoi Plazmy, Moscow: Nauka, 1982. Translated under the title Kinetics of Nonequilibrium Low-Temperature Plasma (New York: Plenum) 1987, 2
Fadeyev, Y. A., & Gillet, D. 2000, A&A, 354, 349
Fadeyev, Y. A., & Gillet, D. 2004, A&A, 420, 423
Fox, M. W., & Wood, P. R. 1985, ApJ, 297, 455
Gorbatskii, V. G. 1961, Soviet Ast., 5, 192
Johnson, L. C. 1972, ApJ, 174, 227
Kaplan, S. A., & Pikel'Ner, S. B. 1979, Fizika Mezhzvezdnoi Sredy (Moskva: Nauka)
Samus, N. N., & Li, Y., RAA (Research in Astronomy and Astrophysics), 2018, 18, 88